Defence Science Journal, Vol. 75, No. 3, May 2025, pp. 278-284, DOI : 10.14429/dsj.20928

Study of Multi-state Phase Gradient Surface with Single Beam Anomalous Reflection for Passive RIS Applications

Sylvie Rana*, Yallanki Sai Sreenija and A.R. Harish

Department of Electrical Engineering, Indian Institute of Technology, Kanpur - 208 016, India
**E-mail: sylvierana21@iitk.ac.in*

ABSTRACT

Reflective Reconfigurable Intelligent Surfaces (RISs) are artifically engineered surfaces that can redirect an incident wave towards any arbitrary direction. As a result, RISs are envisioned to play a significant role in 5G and 6G communications. However, for practical implementation, active RISs may consume significant power besides their complex circuitry, especially when deployed on a large scale. To address this challenge, passive surfaces with nearly continuous phase gradients are being explored as a more efficient alternative. These surfaces consist of periodically arranged arrays of unit cells with linearly varying phase profiles, which can be implemented using two or more unit cells per period. However, using fewer unit cells per period can result in specular reflection besides anomalous reflection. This study demonstrates Phase Gradient Surface (PGS) designs having 18×18-unit cells of two-state to five-state, which effectively redirect incoming waves towards an anomalous direction, with suppressed specular reflection by upto 12.4 dB. They can also adaptively reconfigure the anomalous beam for smaller range of incident angles. Comparative reflection patterns for two- to five-state PGSs are presented, demonstrating that the five-state design achieves the greatest suppression of specular and other undesired reflections, even for incident angle of 20º.

Keywords: Anomalous reflection; Phase gradient surface; Intelligent surface; Reconfigurable intelligent surface

1. INTRODUCTION

Reflective Reconfigurable Intelligent Surfaces (RISs) are widely recognised for their ability to redirect the incident electromagnetic waves toward a non-specular direction (anomalous direction). This phenomenon is achieved by using carefully engineering the surface having multiple unit cells with high reflectivity and a continuous phase distribution, resulting in optimal power transfer towards the desired anomalous direction. Such surfaces with a constant phase gradient are called Phase Gradient Surfaces (PGSs). In PGSs, the number of discrete phase states, which defines the phase gradient, significantly influences the power reflected toward unintended directions including specular direction.

Some researchers have indicated that PGSs can be realized using metasurfaces also called Phase Gradient Metasurfaces (PGMs). Due to their ease of installation and implementation on any flat surfaces, reflective PGMs have been studied extensively for many useful applications like 1-D[1-3] and 2-D[4] beam forming, wavefront control[5-6] etc. The direction of anomalous reflection can be dynamically reconfigured by adjusting the phase properties of the PGM states using active components like PIN or varactor diodes. Thus, PGMs with active elements are often employed to be used as RISs. For instance, two-state programmable PGM equipped with a single diode enables real-time control of various functionalities, including polarization, scattering, focusing[7], and dynamic scattering[8]. A dual-band beam-steering RIS[9] was reported that demonstrated high specular reflection in the lower band, while the higher band showed diminished specular reflections. The beam reconfiguration was accomplished by modifying the states with a single varactor diode. Similar functionality was demonstrated in a two-layer structure incorporating multiple diodes[10], where the higher frequency band showed specular reflections at larger scan angles. Again, a novel RIS design covering entire 5G mm-wave band using optimal coding using 1-bit PIN diode-based switching element to effectively provide beam scanning capability up to 50º[11].

Therefore, metasurfaces with a higher phase gradient (fewer states) are more prone to generating undesired specular reflections, due to abrupt phase changes along their surface. To minimize unwanted reflections, planar loaded antenna arrays have recently been developed to enable precise anomalous reflection in any desired direction by optimising the scattering characteristics of passively loaded array antennas. For a finite-sized fixed array, the deflection angles can be continuously adjusted through appropriate tuning of each load[12-14].

Larger active arrays or antenna arrays with many unit cells can encounter substantial energy losses associated with powering control units and planar loadings. As a result, passive RISs, especially those employing simple rectangular patches as unit cells, have been explored to achieve anomalous reflection in fixed directions, minimizing reliance on active components. Certain anomalous reflectors with a higher number of states have also exhibited specular reflections. For instance, a ten-state anomalous reflector demonstrated higher levels of specular

Received : 10 January 2025, Revised : 03 April 2025
Accepted : 29 April 2025, Online published : 08 May 2025

reflection compared to the anomalous beam[15]. Similarly, an eight-state coding metasurface reflector with a main beam at 75º was found to produce more specular reflection than the ten-state, twelve-state, and sixteen-state configurations, which had main beams reflected at 48º, 38º, and 28º, respectively[16]. Nevertheless, it is feasible to design anomalous reflectors with fewer states while maintaining lower specular reflections. A D-band anomalous reflector can redirect a normally incident wave to angles of 30°, 60°, and 75° using ten, eight, and six distinct states, respectively[17]. These reflectors rely on many states to minimize specular reflections and reflections in undesired directions.

Here we show that with moderate increase in number of states (upto five) in an anomalous reflector, specular reflection as well as spurious higher order modes located at undesired directions can be significantly reduced maintaining a single strong beam towards desired direction. The proposed PGS designs can also reconfigure the direction of anomalous reflections with the change in incident angle, thus making it a good candidate for RIS applications.

2. DESIGN OF PHASE GRADIENT SURFACE

The proposed multi-state PGSs consist of two to five states in each period. Each unit cell, as shown in Fig. 1, consists of a copper-backed FR4 substrate with a thickness of 1.63mm and a size of 15 mm × 15 mm (0.6 λ_0 × 0.6 λ_0), where λ_0 is the operating wavelength. The top copper patch on the unit cell has a variable central gap (g). This unit cell responds well to y-polarized incidence due to its folded dipole-like feature along y-direction. Here, each unit cell represents each state, and different states are distinguished by different central gap values ranging from 0mm to 5mm.

The proposed passive PGS is realized using array of 18 × 18-unit cells (10.8 λ_0 × 10.8 λ_0), as shown in Fig. 2. The periodicity of each case is enlarged and shown below each case of multi-state pass array. Rows of unit cells with the same color represent the same state. The colors on the array are used for illustrative purposes to indicate the different states.

3. WORKING PRINCIPLE

Ideally, PGS based RISs must employ linearly varying phase shifts from 0° to 360° on the reflective surface, which is essential to reflect an incoming incident wave along the desired direction. The continuous phase shifts are often discretized into two or more states to enable practical realization.

When a plane wave impinges on this surface, multiple reflection modes are generated. The direction of propagation of these modes can be represented as the tangential components of their wavenumbers as[18]:

$$k_{r,n} \sin \theta_{r,n} = k_i \sin \theta_i + \frac{2\pi n}{L} \quad (1)$$

where, $k_{r,n}$ and $\theta_{r,n}$ represent the wavenumber and diffraction angle of the n^{th} reflection mode (where n = 0, ±1, ±2, …), k_i is the wavenumber of the incident wave, θ_i is the angle of

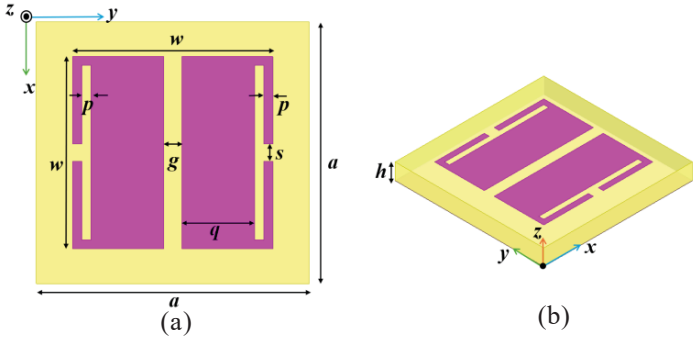

Figure 1. (a) The top view; and (b) Dimetric view of proposed unit cell design. Parameters (in mm): a=15, w=11, p=0.5, q=3.9, g= variable, s=1, h=1.63.

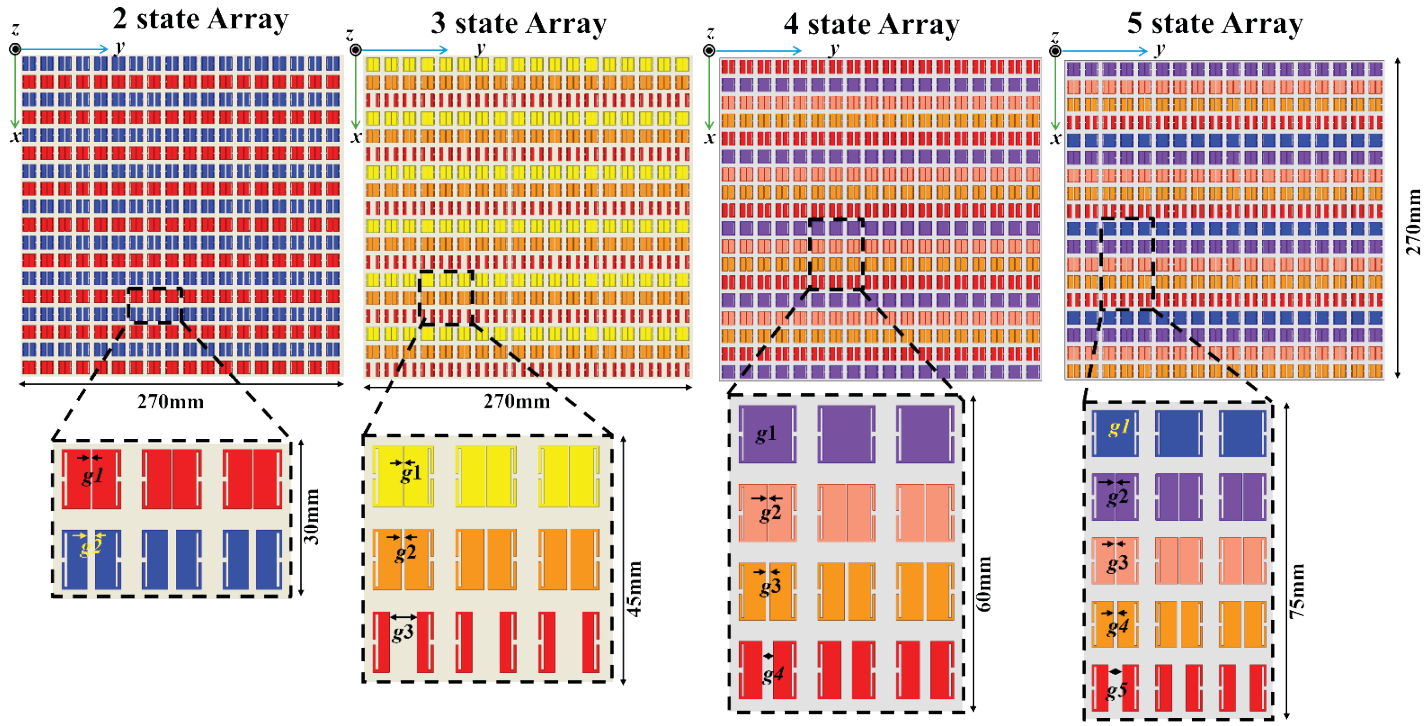

Figure 2. Schematic of multi-state array.

incidence as demonstrated in Fig. 3, and L is the length of one period of the GM, also evident in Fig. 2.

In this work, we will represent θ_i and θ_r as positive when they move away anticlockwise and clockwise respectively, from the normal of the surface in the x-z plane. When both the incident and the reflected waves travel through the same medium, $k_i=k_{r,n}$.

$$\theta_{r,n} = \sin^{-1}\left(\sin\theta_i + \frac{n\lambda_0}{L}\right) \quad (2)$$

For normal incidence (θ_i=0°) and λ_0=25 mm (operating frequency = 12 GHz), the possible propagating modes for multi-state PGSs are calculated in Table 1.

Table 1. Direction of propagating modes for normal incidence on multi-state PGSs

$\theta_{r,n}$	2 state (L=30 mm)	3 state (L = 45 mm)	4 state (L = 60 mm)	5 state (L =75 mm)
$\theta_{r,0}$	0°	0°	0°	0°
$\theta_{r,\pm1}$	±56.44°	±33.75°	±24.62°	±19.47°
$\theta_{r,\pm2}$	-	-	±56.44°	±41.81°
$\theta_{r,\pm3}$	-	-	-	±90°

The direction of propagation of the dominant anomalous reflection mode (here, $\theta_{r,\pm1}$) can be reconfigured by three ways for our proposed PGSs, as predicted from Eqn. (2):

3.1 By Changing the Wavelength

A reduction in the operating wavelength (increase in operating frequency) will lead to shift in the dominant mode towards the normal. Nevertheless, the phase gradient on the PGS must be fairly constant, which may require choosing different values of central gap which will meet the phase gradient criteria.

3.2 By Changing the Periodicity of the PGS

The periodicity of PGS plays the most important role in not only reconfiguring the direction of dominant mode but also eliminating the undesired higher order modes. As the periodicity increases without any change in unit cell size, higher order propagating modes like n=±2 and so on may exist, apart from already present undesired modes. These modes add to power transmission towards undesired direction.

3.3 By Changing the Incident Angle

The most feasible way to reconfigure the direction of dominant mode propagation in a PGS is to change the incident angle. As the incident angle increases, the dominant mode (+1st mode) moves away from the normal towards the +x-axis, it touches the +x-axis and then becomes evanescent. The other undesired higher order modes also follow a similar pattern and may become stronger than the desired mode when they are closer to the normal while the desired mode is closer to the horizon. Thus, in this scenario, it is desirable to operate the proposed structures within incident angles closer to the normal to avoid spurious undesired reflections.

4. SIMULATED RESULTS AND DISCUSSION

The unit cell simulation of the proposed PGS has been carried out in ANSYS HFSS software with Floquet port excitation. Since the unit cell works for y-polarized incidence, the reflection magnitudes and phases for each state of multi-state PGS, achieved by choosing appropriate central gap values are tabulated in Table 2. The simulated magnitude for each state shows to be higher than -3dB, representing high reflectivity for the operating frequency of 12GHz. The reflection phases show corresponding phase gradients of 180º, 120º, 90º and 72º for two-, three-, four- and five-state PGSs respectively.

The proposed PGSs have been simulated with FEBI (Finite Element Boundary Integral) boundaries and plane wave incidence normally (θ_i=0°) on the multi-state patterned surfaces. The scattered fields are plotted as normalized bistatic RCS on x-z plane (ϕ=0°), as shown in Fig. 3 for multi-state cases. The n=+1 modes were seen at +56°, +34°, +25° and +20°, for two-state to five-state cases respectively. As predicted from Table 1, the other undesired reflection modes are also present with suppression.

The specular reflection (at θ_r=0°) is seen to be the highest for two-state case and gradually decreases with the increase in the number of states. For the five-state case, the amplitude of the specular reflection is 12.4dB lower than the amplitude of the beam at +20°. With the progressive increase in the number of states in a PGS, the phase gradient becomes smaller and thus the phase profile becomes smoother along the direction of applied gradient, which tends to represent a continuous and linear phase profile. Abrupt phase changes along the PGS gives rise to stronger undesired direction reflection, along with specular reflections. Hence, with our proposed design, the

Table 1. Simulated reflection coefficients of unit cell for multi-state cases

g (mm)	Reflection coefficient	
	Magnitude (dB)	Phase (º)
	2-states	
0.28	-1.49	-104.19
1.5	-0.73	74.66
	3-states	
0.21	-1.17	-122.21
0.7	-1.9	-2.49
5	-0.13	117.12
	4-states	
0	-0.22	177.82
0.33	-1.7	-91.16
0.7	-1.98	-2.14
2.1	-0.43	93.16
	5-states	
0	-0.22	177.82
0.27	-0.75	-144.89
0.5	-2.15	-45.43
1	-1.33	41.77
3.4	-0.21	109.19

Table 3. Suppression in Specular Reflection for Distinct state of PGS

Number of states	Direction of maxima (º)	Suppression in specular reflection (dB)
2	±56.44	1.97
3	+33.75	7.11
4	+24.62	8.21
5	+19.47	12.4

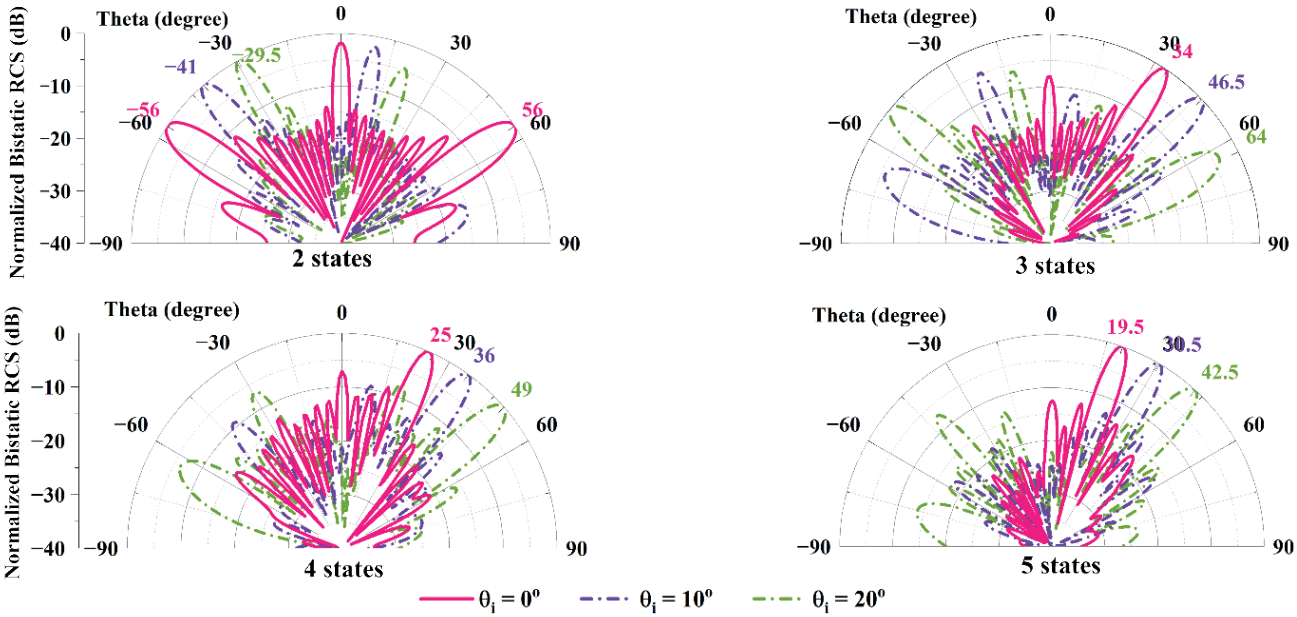

Figure 3. Simulated normalized bistatic RCS plots of multi-state PGS for y-polarized normal, 10º and 20º incidences. (Positive angle towards +x axis for ϕ=0° and towards +y axis for ϕ=90°).

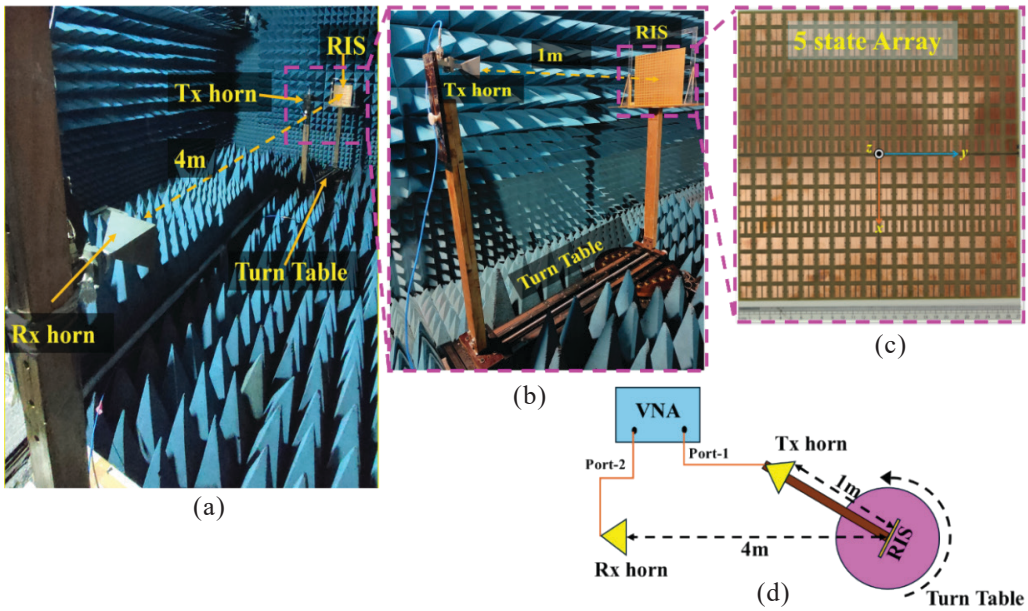

Figure 4. (a) Measurement setup; (b) Enlarged view of setup on turn table; (c) Fabricated structure (five-state array); and (d) Schematic representation of the measurement setup.

increase in number of states will show not only a reduction in specular reflections, but also other undesired propagating modes. The suppression of the specular reflection with respect to the main propagating mode is tabulated in Table 3.

On the other hand, Fig. 3 also shows that the n=-1 mode, for two-, three-, four- and five-state cases, is also present with a suppression of 0 dB, 13.22 dB, 13.18 dB, and 22.45 dB respectively at their expected directions. Presence of other higher order propagating modes like n=±2 is also weakly visible at their respective directions. Thus, as the number of states increases, the generation of spurious undesired propagating modes is inevitable.

The scattering patterns for higher incident angles of 10° and 20° are also plotted on Fig.3. It is evident that for each multi-state case, except the two-state case, the dominant mode moves away from the normal for increase in incident angle. For the two-state case, the dominant mode is evanescent when the incident angle is greater than 9.59º. Therefore, in Fig. 3, the dominant mode is not visible for incident angles of 10º and 20º. The other higher order modes also follow the same pattern, but they tend to be stronger as they approach the normal. Even for a higher incident angle of 20º, this phenomenon could be reduced subsequently as the states are increased to five where only n=-3 mode located at -41º is found to be strong. All the other undesired modes are successfully pushed below 10dB than the dominant mode. Interestingly, for three-state case we do notice the undesired n=-2 mode located at -50º shoots up above the desired mode, which can significantly hinder the

PGS performance. Thus, it might be ideal to operate lower state designs with lower incident angles to avoid the same.

5. MEASUREMENT SETUP AND RESULTS

The proposed multi-state PGSs are fabricated using separate FR4 substrates of same size of 270 mm × 270 mm × 1.63 mm each. Scattering pattern measurements of these structures are conducted in an anechoic chamber. As shown in Fig. 4(a), the measurement setup consists of two X-band horn antennas, one serving as the transmitter and the other as the receiver, and the fabricated PGS, mounted on the axis of a turn table. The transmitting antenna is placed at 1m distance from the PGS, aligned normally to the PGS. The enlarged view of the setup on the turn table is shown in Fig. 4(b). Port-1 and port-2 of a vector network analyzer (VNA) are connected to the transmitting horn and the receiving horn, respectively. A photograph of the fabricated five-state array is shown in Fig. 4(c).

To measure the reflected power, the receiving horn is placed at approximately 4 meters away from the PGS. The turn table, along with PGS and the transmitter horn mounted on it, is rotated from -90° to +90°, to record the S_{21} parameter on the VNA. Due to the limitations of the turn table and space constraints of the anechoic chamber, the horn antennas could not be placed in the far-field region of the PGS, which is approximately 11 meters. The schematic representation of the entire measurement setup is illustrated in Fig. 4(d) for better understanding.

To replicate the measurement setup, the simulation of each multi-state array is carried out with an X-band horn as source located at 1m from the PGS. The normalized gain patterns are then compared with the measured patterns.

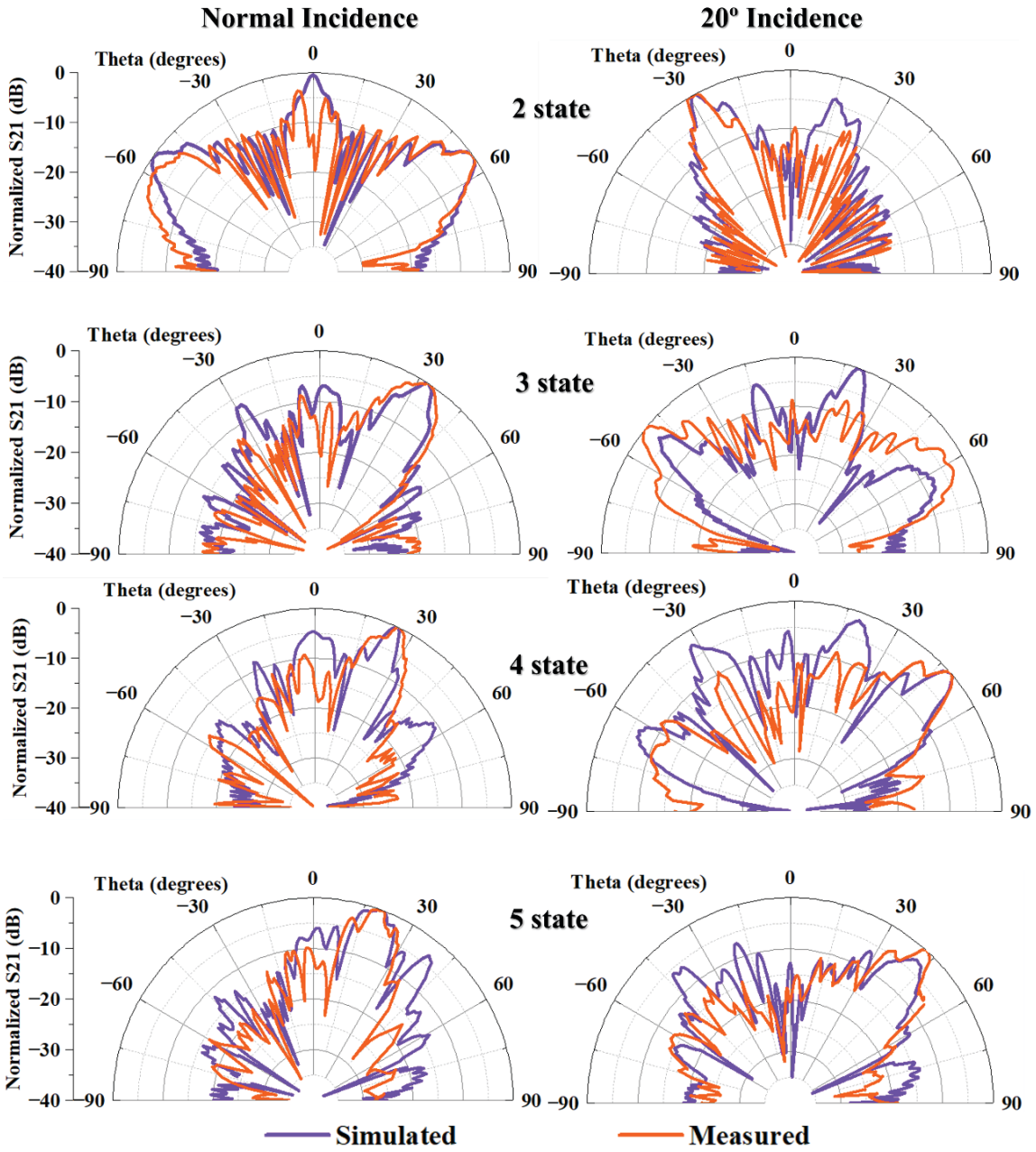

Figure 5. Measured Results for Normal incidence and 20º incidence on the proposed multi-state PGSs.

For normal incidence, progressive suppression of the specular reflection (θ_r=0°) are seen as we increase the number of states for each passive PGS design. The anomalous reflection is found to be strong for all cases at the expected directions. Despite, the measured pattern showing a null for all cases particularly at θ=0°, the overall beam is seen to have been suppressed progressively. The null at 0º seems to be due to horn blocking the received signal in that direction, however more investigation needs to be carried out to avoid such dip in response. The measured 3dB beamwidths are 9º, 12º ,6º and 7º for two- to five-state arrays for normal incidence, respectively, which are slightly wider than the simulated cases due to the nulls getting filled.

For 20º incidence, the main anomalous beam is found to exist along the directions as predicted by the simulations. However, the undesired reflection beams seen in simulation are supressed significantly in the measured results. For the three-state case the amplitude of the n=-2 mode is higher than that of the n=+1 mode, as predicted by the simualtion. The discrepancy between the measured and the simulated results, in particular for the negative higher order modes needs further investigation.

6. CONCLUSION

In this work we demonstrate periodic multi-state passive phase gradient surface that provide anomalous reflection. The unit cell design is simple, with distinct states represented by variations in a single parameter. We demonstrate that increasing the number of states in an anomalous reflector substantially reduces specular reflection while preserving a strong beam in the desired direction, achieving a maximum specular reflection suppression of 12.4 dB for the five-state case. The anomalous reflection direction can be reconfigured for each of the multi-state designs by changing the angle of incidence.

Owing to their ease of fabrication and minimal design complexity, the proposed surface designs are ideal for connecting to stationary targets located in blind spots when the PGS is positioned normal to the signal source. They are also well-suited for scenarios requiring multi-target connectivity, such as densely populated areas served by a single base station or providing seamless and simultaneous connectivity to multiple satellites using a cost-effective setup.

REFERENCES

1. Díaz-Rubio, A. & Tretyakov, S. A. macroscopic modeling of anomalously reflecting metasurfaces: Angular response and far-field scattering. *IEEE Transact. on Antennas and Propag.*, 2021, **69**(10), 6560-6571. doi: 10.1109/TAP.2021.3076267.
2. Liang, J.C.; Cheng, Q.; Gao, Y.; Xiao, C.; Gao, S.; Zhang, L.; Jin, S. & Cui, T.J. An angle-insensitive 3-bit reconfigurable intelligent surface. *IEEE Transact. on Antennas and Propag.*, 2022, **70**(10), 8798-8808. doi: 10.1109/TAP.2021.3130108.
3. Malleboina, R.; Dash, J.C. & Sarkar, D. Design of anomalous reflectors by phase gradient unit cell-based digitally coded metasurface. *IEEE Antennas and Wireless Propag. Lett.*, 2023, **22**(9), 2305-2309. doi: 10.1109/LAWP.2023.3287031.
4. Zhang, N. et al. Programmable coding metasurface for dual-band independent real-time beam control. *IEEE J. Emerging and Selected Topics in Circuits and Syst.*, 2020, **10**(1), 20-28. doi: 10.1109/TAES.2024.3443793
5. Mohammadi, N. & Alu, A. Wave-front transformation with gradient metasurfaces. *Physical Rev. X*, 2016, **6**, 041008. doi: 10.1103/PhysRevX.6.041008.
6. Ill, D.B.; Lawrence, M. & Dionne, J. Wavefront shaping and modulation with resonant electro-optic phase gradient metasurfaces. *Appl. Phys. Lett.*, 2021, **118**, 071104. doi: 10.1063/5.0038842.
7. Yang, H.; Cao, X.; Yang, F.; Gao, J.; Xu, S.; Li, M.; Chen, X.; Zhao, Y.; Zheng, Y. & Li, S. A programmable metasurface with dynamic polarization, scattering and focusing control. *Sci. Rep.*, 2016, **6**, 35692. doi: 10.1038/srep35692.
8. Wan, X.; Qi, M.Q.; Chen, T.Y. & Cui, T.J. Field-programmable beam reconfiguring based on digitally-controlled coding metasurface. *Sci. Rep.*, 2016, **6**, 20663. doi: 10.1038/srep20663.
9. Lin, H.; Yu, W.; Tang, R.; Jin, J.; Wang, Y.; Xiong, J.; Wu, Y. & Zhao, J. A dual-band reconfigurable intelligent metasurface with beam steering. *J. Phys. D: Appl. Phys.*, 2022, **55**, 245002. doi: 10.1088/1361-6463/ac5663
10. Zhang, N.; Chen, K.; Zheng, Y.; Hu, Q.; Qu, K.; Zhao, J.; Wang, J. & Feng, Y. Programmable coding metasurface for dual-band independent real-time beam control. *IEEE J. Emerg. and Selected Topics in Circuits and Syst.*, 2020, **10**(1), 20-28. doi: 10.1109/JETCAS.2020.2970963.
11. Wang, R.; Yang, Y.; Makki, B. & Shamim, A. A wideband reconfigurable intelligent surface for 5g millimeter-wave applications. *IEEE Transact. on Antennas and Propag.*, March 2024, **72**(3), 2399-2410. doi: 10.1109/TAP.2024.3352828
12. Vuyyuru, S.K.R.; Valkonen, R.; Kwon, D.-H. & Tretyakov, S.A. Efficient anomalous reflector design using array antenna scattering synthesis. *IEEE Antennas and Wireless Propag. Lett.*, 2023, **22**(7), 1711-1715. doi: 10.1109/LAWP.2023.3287031.
13. Vuyyuru, S.K.R.; Valkonen, R.; Tretyakov, S.A. & Kwon, D.-H. Modeling RIS from electromagnetic principles to communication systems--part i: Synthesis and characterization of a scalable anomalous reflector. *arXiv preprint arXiv:2403.12790*, 2024, 1-10. doi: 10.48550/arXiv.2403.12790.
14. Vuyyuru, S.K.R.; Valkonen, R.; Tretyakov, S.A. & Kwon, D.-H. Efficient synthesis of large finite patch arrays for scanning wide-angle anomalous reflectors. *IEEE Open J. Antennas and Propg.*, 2024. doi: 10.1109/OJAP.2024.1234567.
15. Díaz-Rubio, A.; Asadchy, V.S.; Elsakka, A. & Tretyakov, S.A. From the generalised reflection law to the realization of perfect anomalous reflectors. *Sci. Adv.*, 2017, **3**, 1602714.

doi: 10.1126/sciadv.1602714.
16. Jing, H.B.; Ma, Q.; Bai, G.D. & Cui, T.J. Anomalously perfect reflections based on 3-bit coding metasurfaces. *Adv. Opt. Material.*, 2019, **7**, 1801742. doi: 10.1002/adom.201801742.
17. Kato, Y.; Omori, K. & Sanada, A. D-band perfect anomalous reflectors for 6g applications. *IEEE Access*, 2021, **9**, 157512-157521. doi: 10.1109/ACCESS.2021.3130058
18. Qi, C. & Wong, A.M.H. Discrete huygens' metasurface: Realizing anomalous refraction and diffraction mode circulation with a robust, broadband and simple design. *IEEE Transact. on Antennas and Propag.*, 2022, **70**(8), 7300-7305. doi: 10.1109/TAP.2022.3164931

ACKNOWLEDGEMENT

The authors express gratitude to the High-Performance Computing (HPC2013), Indian Institute of Technology, Kanpur for providing access to the necessary nodes for simulations.

CONTRIBUTIONS

Ms. Sylvie Rana is currently pursuing her PhD from IIT, Kanpur. Her research interests include: Anomalous reflection and transmission from phase gradient surfaces, reconfigurable intelligent surfaces, polarization converters, and polarization-selective absorbers using metasurfaces.
In the current study she carried out the simulations, analysis, measurements, and paper writing for this work.

Ms Yallanki Sai Sreenija obtained her Master's degree from the IIT, Kanpur. Her research interests include: Antennas, antenna arrays, metasurfaces and RF measurements.
In the current study she provided valuable insights for this work and contributed significantly to the fabrication and measurement of the proposed structures.

Prof A.R. Harish is a Professor at the IIT, Kanpur. His research interests include: Antenna, antenna arrays, shared aperture antennas, metamaterials, reconfigurable intelligent surfaces etc. He supervised this work and provided valuable insights to improve and finalise it.